Hindawi
Journal of Nanotechnology
Volume 2022, Article ID 5882113, 11 pages
https://doi.org/10.1155/2022/5882113

Research Article

Comparing Acid and Enzymatic Hydrolysis Methods for Cellulose Nanocrystals (CNCs) Obtention from Agroindustrial Rice Husk Waste

Ricardo Hernández Pérez, René Salgado Delgado, Alfredo Olarte Paredes, Areli Salgado Delgado, Edgar García Hernández, Atenas Medrano Valis, and Fryda Martínez Candia

[1]*National Technological Institute of Mexico/Technological Institute of Zacatepec, Road No. 27, Col. Center, Zacatepec, Morelos 62780, Mexico*

Correspondence should be addressed to Ricardo Hernández Pérez; santaclara57@yahoo.es

Received 27 May 2022; Revised 31 October 2022; Accepted 23 November 2022; Published 6 December 2022

Academic Editor: Marco Rossi

Agroindustrial residues represent a serious environmental problem in the world; in this case, the polluting rice husk, present in the rice fields of Morelos State, is one source of incalculable biomass. The aim of this study was to assess two viable and optimized procedures for obtaining nanocellulose from these wastes. The sieved samples included 4 treatments with different grain sizes (sieves # 10, 15, 30, and 50) and three replicates. They were then processed by an alkaline treatment (NaOH) 5%, bleaching with sodium hypochlorite, followed by pretreatment with 0.65% hydrochloric acid (HCl). After drying, the cellulose was subjected to acid hydrolysis with (H_2SO_4) at 64%, and was compared to an enzymatic hydrolysis complex. This complex was formed of D-(+) cellobiose and endo-1,4-β-D-glucanase from Acidothermus cellulolyticus. End products were sonicated and dialyzed until they reach a neutral pH. Finally, the nanocellulose was characterized by FTIR, DSC, XRD, SEM, and TEM. Evident results recognize the nanocellulose (NC) synthesis by both routes, with greater contaminants generated in the medium by the acid hydrolysis. It is much more feasible and faster to achieve with enzymatic hydrolysis, less aggressive for the environment, and higher performance. In future trials, the cost-benefit of using the enzyme complex should be assessed as an alternative to replace acid hydrolysis.Key words: acid hydrolysis, enzymatic hydrolysis, waste, rice husk, Oryzasativa L, cellulose nanocrystals (CNCs).

1. Introduction

It is well known that the current economic system is based on a society of intensive consumption and the indiscriminate use of fossil fuels. This compromises the future of life on the planet and has disastrous consequences for climate change. In this context, the development of new lines to produce biofuels and bioproducts from renewable sources and less expensive biomass represents an alternative or key way to make an economic transition from the indiscriminate use of oil, to a new bioeconomy where processes are developed. It is more efficient and sustainable, from the recycling of waste from the agricultural industry [1].

Natural fibers have been incorporated into different technologies and applications, which include the car industries, food, and agricultural, due to the large quantity and diversity of biomasses that originate a resistant, sustainable, and low-cost material. By incorporating various nanotechnological materials, an emerging industry arises, related to textiles or metals, creating new products with high added value. Some examples are as follows: nanofibers, carbon tubes, and silver nanoparticles [2, 3]. The availability of these materials and their

application in nature have been the stimulation to try more with vegetable fibers. Rice husk, for example, is an abundant contamination waste in the field, which has a low price and a big future as a material for this industry [3]. However, the composition of rice husk is more complex than that of other fibrous materials. The silica, which is 91.1% distributed in the rice husk, occurs as hydrated grains, which are biosynthesized through the polymerization of silica acid, given the activity of microorganisms [4–6].

Morelos is among the seven largest rice producers in Mexico, with more than a thousand tons Frenot et al. [7]. Currently, cellulosic agricultural waste materials that are sustainable, green, and environmentally friendly [8] have been widely used as sources for nanoparticle extraction [9, 10]. Different processes have been tested from various sources, such as wood residues, paper [11, 12], as well as from the rice husk itself [13–24]. Recent studies reported the possibility of using acid hydrolysis to obtain cellulose whiskers by treating rice hulls from milled long grain with improved yield [25].

Previous results clarified that to treat the rice husk (RH), before cooking with KOH, it was more convenient to do a pretreatment with 10% HCl (v/v). In the end, this managed to reduce the size of the nanoparticles (26 to 29 nm) and increase the crystallinity of nanocellulose (70.9), unlike when using rice straw (RS) [3, 26]. On the other hand, a greater use of the treated biomass was obtained, previously eliminating a greater number of macromolecules, which offers greater cellulose yield when sieved between (10–30) was used, achieving a cellulose better prepared for the next acid hydrolysis [25].

Some studies have achieved the preparation of nanocellulose particles using ionic liquid (BmimHSO4) synthesized at 90°C, which offers a simple and environmentally friendly approach as ionic liquid can regenerate and is reusable [2].

From the advances achieved with some varieties of rice (*Oryza sativa* L.) and its straw in Morelos state, the objective of comparing the effectiveness of acid hydrolysis against a simple enzyme complex to obtain cellulose nanocrystals (CNCs) was proposed.

2. Materials and Methods

2.1. Experimental Materials

(i) NaOH, CAS: 1310-73-2, ALDRICH.

(ii) HCl, CAS: 7647-01-0, ALDRICH.

(iii) H_2SO_4 CAS: 7664-93-9, ALDRICH

(iv) $NaClO_2$ CAS:7758-19-2, ALDRICH.

(v) C7253-10MG D-(+) cellobiose SIGMA-ALDRICH.

(vi) E2164-100UN. endo-1,4-β-D-glucanase from *Acidothermus cellulolyticus.* SIGMA-ALDRICH

(vii) Dialysis tubing, high retention seamless cellulose tubing. avg. flat width 23 mm (0.9 in.), MWCO 14000, 99.99% retention.

(viii) Pur-A-Lyzer™ Maxi Dialysis Kit. Maxi 12000, capacity 0.1–3 mL, pkg of 50 Maxi dialysis tubes, MWCO 12–14 kDa.

2.2. Native Biomass. In previous analysis, the composition of the native biomass used was found which consist of the following: lignin (7.68%), hemicellulose (16.98%), holocellulose (53.8%), ash (21.9%), silica (70.6%), and cellulose (36.8%). Corroborated data with the bibliography indicate that they were acceptable for rice husk [3, 10, 27].

2.3. Methods

2.3.1. Biomass Preparation. Wevisited the rice mill in Cuautla that produces the brand "Buena Vista" in Morelos State, where the sample of rice husk was obtained, as raw material for synthesis. The sample was taken to the Laboratory. of Chemistry Engineering at the Technology Institute of Zacatepec (ITZ), where the extraction protocol was followed. The rice husk was thoroughly washed with stirring at temperature of 65°C for 1.30 h, with water distilled to remove foreign materials. It was then dried and stored in an auxiliary container made of airtight glass to prevent the contamination of microorganisms. For the trial, the husk was crushed into finer particles, for which a common blender was used, and then passed through sieves # 10, 15, 30, and 50, forming four treatments and three replicas [22, 25].

2.3.2. Cellulose Extraction. The cellulose extraction had three steps: alkaline chemical treatments, cellulose bleaching, and acid pretreatment, to a heavy and drying end.

2.3.3. Alkaline Treatment. The chopped, ground, and sieved rice husk was subjected to alkaline treatment, using 20 g per treatment, testing three concentrations of sodium hydroxide NaOH 5%, with a husk liquor ratio of 1 : 10 at different temperatures of 102, 110, and 113°C, respectively, and a cooking process of 90 min. The insoluble residue of rice husk after heating was left to stand (20 min.) to cool, then filtered and washed with abundant distilled water. Finally, it was dried on the stove at 80°C for 3 h, and once dried, its weight was recorded. This procedure mainly allowed the removal of lignin and the elimination of excess NaOH [22, 28].

2.3.4. Bleaching Treatment. To remove lignocellulosic residues, had necessary by a bleaching process, using sodium hypochlorite ($NaClO_2$), at 1% in a ratio (50 : 1) of liquor for bleaching. The mixture was constantly stirred to 80°C for 2 h.

Later, the mixture was allowed to cool and leak, while distilled water was added, until the pH of the solution reached neutral. Subsequently, it was dried on the stove at 80°C for 3 h, and a record of its weight was made [23, 28].

2.3.5. Acid Pretreatment. Pretreatment with HCl at 0.65% was necessary to remove other macromolecular components such as hemicellulose. After mixing 20 g of cellulose, the acid was applied (100 mL) under stirring at 80°C for 1.5 h. Finally, the biomass was washed with distilled water until reaching neutral pH and was dried at 80°C for about 3 h [21].

2.4. Nanocellulose Obtention

2.4.1. Acid Hydrolysis. Once the quality of the cellulose was characterized, acid hydrolysis was performed to achieve its reduction and obtain nanocellulose. For hydrolysis, 64% sulfuric acid (H_2SO_4) was used with a cellulose/acid ratio of 1/10 (w/w) concentration, with reaction time of 45 min at 45°C temperature and constant agitation [28]. Once the time had elapsed, the mixture was cooled by adding 650 mL of distilled water to stop the reaction. Subsequently, it was allowed to settle, and a decantation was made, leaving the supernatant. This process was repeated until the sedimentation time of the mixture was longer. This mixture was transferred to a flask (50 mL) and placed in an ultrasonic bath at 30 (KHz) of amplitude to completely separate the crystalline part of the amorphous, where we waited to observe two phases in the bottle: a sediment (microfibers) at the bottom and the supernatant (nanocrystals) [4, 17]. In this case, the supernatant was taken, which was washed by several centrifugation cycles at 3600 rpm for 30 min. In each change, the precipitate of the tubes was diluted with sterile water, the acidity was recorded, and repeating the centrifugation cycles and changes with water, until reaching neutral pH [15, 29].

2.4.2. Enzymatic Hydrolysis. The assay was carried out using an enzymatic complex composed of D-(+) cellobiose (SIGMA-ALDRICH) and endo-1,4-β-D-glucanase from *Acidothermus cellulolyticus* (SIGMA-ALDRICH). They were applied in tow phase on the samples. First, a stock solution of each enzyme was prepared, taking into account the activity suggested by the manufacturer, at a final concentration of 5 mg/50 mL for the first and 1 mg/50 mL for the second.

Each cellulose sample (5 g) was treated with 1 mL of the stock solution of the cellobiose enzyme for 72 h at a temperature of 50°C under constant agitation. At the end, it was left to cool for 24 h at rest. It was verified that the pH was maintained between 4 and 5 [30]. The second enzyme was then applied at a rate of 1 ml and left for 72 h at room temperature. Finally, the sample was brought to neutral pH with sterile water, and once neutrality was reached, the supernatant was taken and treated with an ultrasonic bath at 28 Hz/30 min. At the end, it was centrifuged at 3600 rpm/10 minutes to concentrate the nanoparticles [30, 31].

2.5. Characterization and Functional Groups

2.5.1. Infrared Spectroscopy with Fourier Transform (FTIR). A spectroscopic analysis of FTIR with Fourier transform on the treated fibers was performed to evidence the effect of this on the hemicellulose and lignin contained in the fibers. A Perkin Elmer FTIR spectroscopy equipment was used, using 16 scans in a range of 600–3800 cm^{-1}.

2.5.2. Scanning Electron Microscopy (SEM). A morphological analysis was performed using scanning electron microscopy (SEM) with a team JEOL brand model JSM-6010 LA, in which the samples were prepared in vacuum and coated with gold to avoid static load and operated at 20 kV. The morphological analysis will be performed both on the surface and the ends of the microfibers and nanocrystals. Working conditions were described by [32, 33].

2.5.3. Transmission Electron Microscopy (TEM). A transmission electron microscope (TEM) from the National Autonomous University of Mexico (UANM) marked JEOL JEM-140, operating at a voltage of 120 kV, was used to assess the surface morphology and dimensions of the nanoparticles. A drop of aqueous suspension was deposited on a copper grid (360 meshes) and allowed to dry under vacuum. The copper grid was then inserted into the instrument, and images of the nanocellulose particles were captured under different magnifications [34].

2.5.4. Differential Scanning Calorimetry (DSC). The DSC thermal analysis was carried out in collaboration with the Autonomous University of Hidalgo for all treatments. The crystallization process of these materials was evaluated by differential scanning calorimetry, and the samples were sealed in aluminium capsules of 40 mL; these were carried from −40 to 300°C at a heating rate of 5°C/min. Subsequently, to remove the thermal history, they will be quickly cooled to −40°C at a speed of 30°C/min and subsequently brought up to 180°C at the same heating rate [25, 32].

2.5.5. X-Ray Diffraction (XRD). X-ray diffraction patterns were obtained using an X-ray diffractometer at room temperature with a monochromatic CuKα radiation source in the step-up scan mode with 2θ ranging from 10° to 50° with a step of 0.04 and a scanning time of 5.0 min. Each material in the form of milled powder was placed on the sample holder and leveled to obtain total and uniform X-ray exposure. The crystallinity index (CrI) was measured by Segal's method [4] with an equation as follows:

$$\mathrm{CrI}\,(\%) = \frac{I002 - I\mathrm{am}}{I002} \times 100, \quad (1)$$

where (I002) is the maximum intensity of the diffraction of the (002) lattice diffraction peak and (Iam) is the intensity value for the amorphous cellulose. The diffraction peak is located at a diffraction angle of around $2\theta = 22°$ and the intensity scattered by the amorphous region is at a diffraction angle of around ($2\theta = 18°$).

3. Results and Discussion

3.1. Cellulose Yield. Results on obtaining cellulose from different grain sizes, applying a cooking process with (NaOH 5%) and pretreatment with HCl, are shown (Figure 1).

Evidently, the size and processing are carried out with (NaOH) 5%, influenced to final yield.

When comparing the yield of cellulose obtained from different treatments, the size of the grain after grinding rice husk favored the cellulose yield. Both treatments (T2) and (T3) with particle size (sieves # 15 and 30), respectively, were different from the others in the three phases of the process.

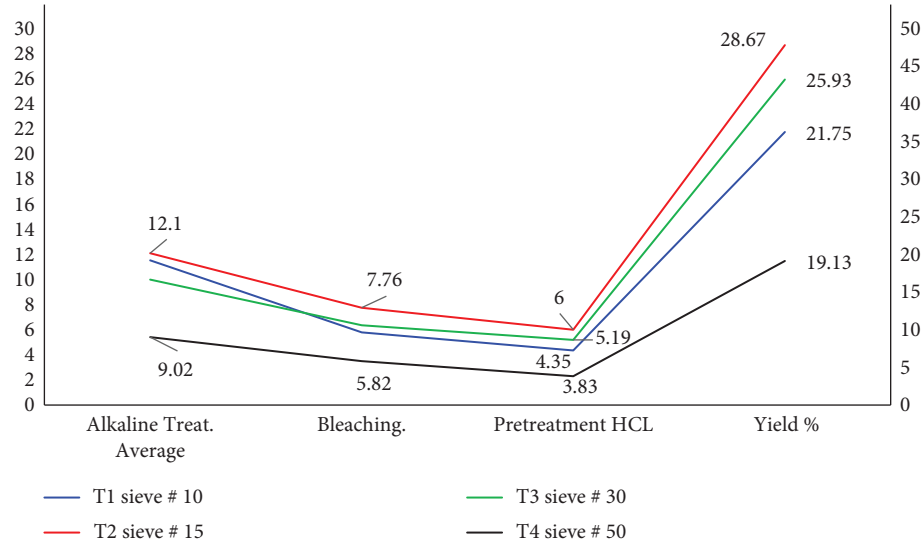

Figure 1: Averages obtained in cellulose yield with different sieves, cooking using alkaline treatment (NaOH) 5%, bleaching, and pretreatment HCl. Treatments T1 (sieve # 10), T2 (sieve # 15), T3 (sieve # 30), and T4 (sieve # 50). (source: author himself).

Showing a greater loss of biomass when bleaching is carried out and finally in acid pretreatment, influencing the smaller grain size T4 (sieve # 50).

The number of washes to reduce the pH and decantation produced cellulose losses, both when the grains were very fine or when coarser grains were used in the three stages.

The highest percentage value of cellulose (28.6%) coincides with reports by other authors who achieved between 28–36% [4, 25, 27, 35–37], but minor to others that obtained greater quantity 41% [38].

3.2. Scanning Electron Microscopy (SEM). Observations denote the structure of fiber packets, which are separated individually, typical of the rice husk when it is being broken down, the decrease in noncellulosic components, which are produced by the separation of the primary wall cell, and as a consequence, the elimination of hemicellulose and lignin is achieved (Figure 2). This corroborates the statements of other authors who have used alkaline treatment followed by acid pretreatment [21].

The smooth appearance of the internal surface of this used material and the rougher external surface, with the formation of linear striated ridges, were also confirmed [10, 13, 25, 33].

Some cellulose samples characterized by Fourier transform infrared spectroscopy (FTIR) showed the effect of grain size. Figure 3 indicates some signals of functional groups such as ester, ketone, and alcohol. When rice husk biomass was used, some peaks were shown between 3050–3600 cm^{-1}, related to O-H bonds [19, 25, 39], aliphatic C-H extending from 2850 to 2999 cm^{-1}, as well as the bending of H bridges from 1600 to 1650 cm^{-1}. It also presents an important peak corresponding to a bending of C-H bridges between 1380 and 1500 cm^{-1}.

Finally, a peak was observed with a signal from the O-H group between 670–625. Such functional groups have been previously declared by other authors [13, 17, 25, 32, 40].

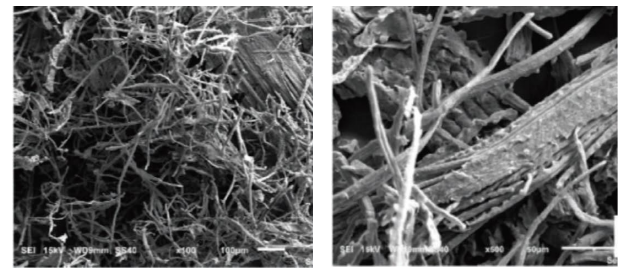

Figure 2: Cellulose images obtained from rice husks and taken under scanning electron microscopy (SEM), coated with colloidal gold, are shown as follows: on the left, treatment with 10 grain mech, amplified × 100 (100 μm), on the right, shows with grain 30 mech amplified × 500 (50 μm). (source: author himself).

3.3. Nanocellulose Characterization

3.3.1. Fourier Transform Infrared Spectroscopy (FTIR). The FTIR spectra corresponding to nanocellulose obtained after enzymatic hydrolysis are shown (Figure 4). The broadband, generated in the region of 3330 cm^{-1}, indicates the stretch vibration of the OH groups.

This increase can be attributed to the greater number of OH groups exposed by the treatment in obtaining the nanocellulose [16]. Visualized also a peak to 2920 cm^{-1} corresponded to asymmetric- symmetric tension C-H. Also was corroborated that from 1650 cm^{-1} appear the OH groups of adsorbed water (hydrogen bonds) and the vibrations in the peaks of 1200–930 cm^{-1} corresponds to stretching of C-O, attributed to the hemicellulose formed in the chemical treatment, like was indicated [32, 41].

Coinciding with the previous analysis, treatments 2 and 3 with medium grain size offered the best results with enzymatic hydrolysis [10].

The FTIR spectra corresponding to nanocellulose obtained after acid hydrolysis are shown (Figure 5). The bands

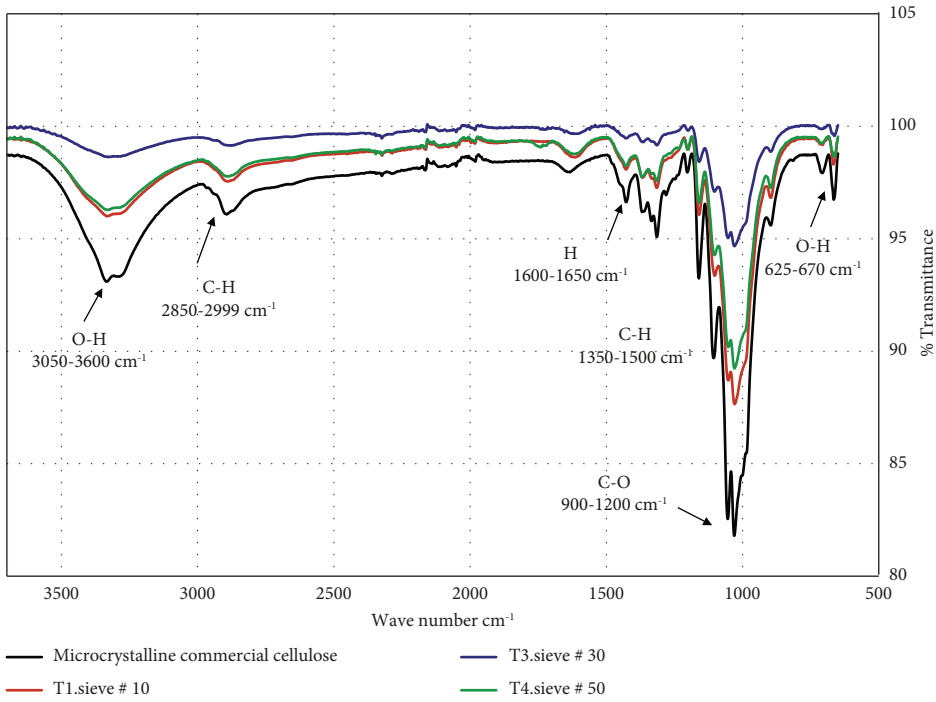

Figure 3: Cellulose comparison extracted from rice husk and characterized by Fourier transform infrared spectroscopy (FTIR). Commercial standard and three treatments cellulose samples processed with NaOH 5% and sieves # 10, 30, and 50. (source: the author himself).

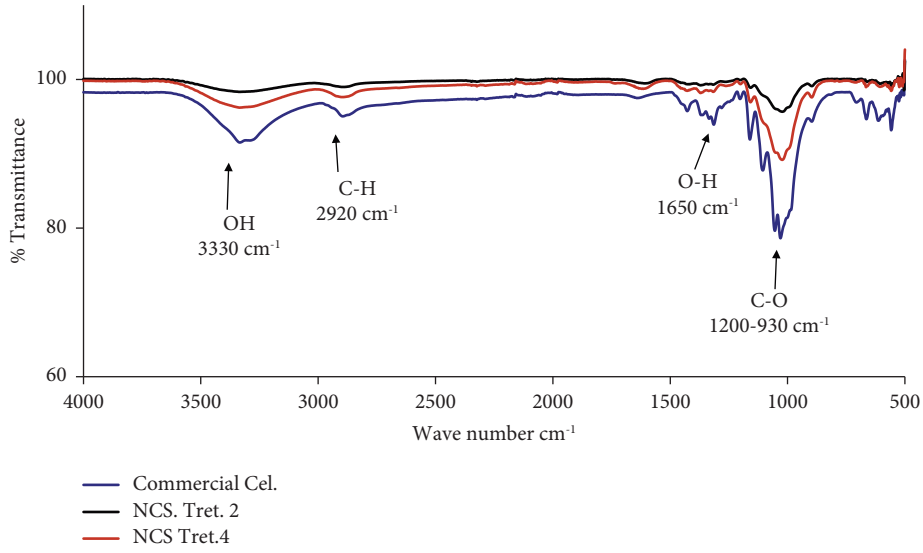

Figure 4: Nanocellulose comparison obtained by enzymatic hydrolysis (NC) from rice husk, characterized by Fourier transform infrared spectroscopy (FTIR). (NCS tret.2) and (NCS tret 4). (source: the author himself).

generated were very similar to the groups found when enzymatic hydrolysis was applied.

However, some particularities regarding the non-uniformity between treatments *T*4 and *T*3 were observed, when H_2SO_4 was used. On the enzymatic pathway, there are no sharp transitions, and the peaks originating between them are very similar and soft.

Noteworthy are the peaks formed at 2920 cm^{-1} and 1650 cm^{-1} with greater bound water in the treatment 4.

It has been reported that the chemical treatments described eliminate lignin with the disappearance of the stretch signal $C=O$, 1732 cm^{-1} [16, 17], in addition to the elimination of hemicellulose macromolecules since changes attributed to ester groups are reported for uronic and acetyl hemicelluloses or ester bonds of carboxylic groups of ferulic acids or lignin p-coumaric [13]. The cellulose samples obtained in the treatments were compared with commercial crystalline cellulose by infrared spectroscopy with Fourier transform (FTIR).

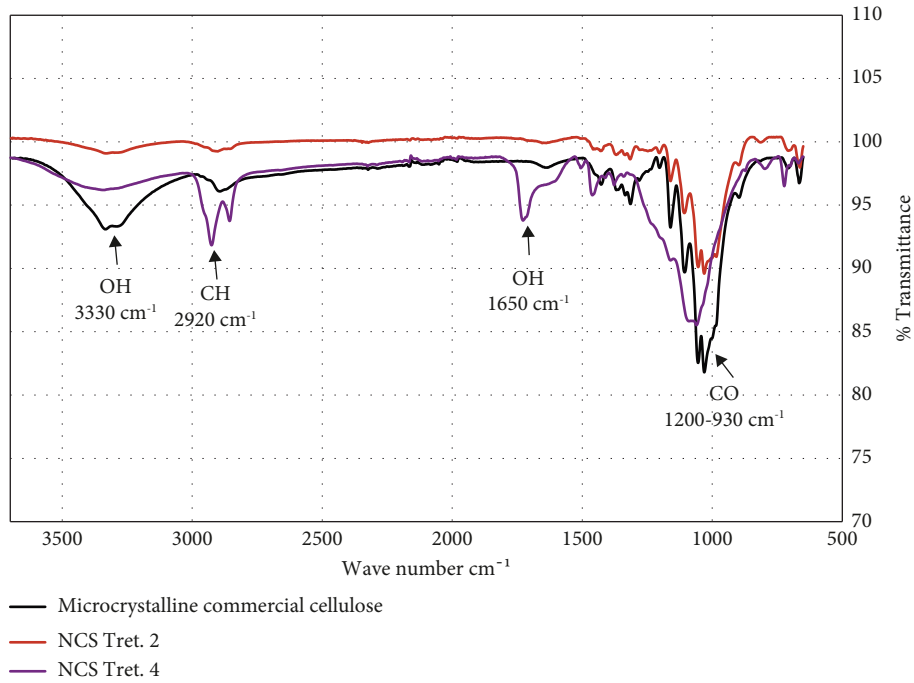

Figure 5: Nanocellulose comparison obtained by acid hydrolysis from rice husk characterized by Fourier transform infrared spectroscopy (FTIR). (Nanocellulose tre. 2. and tret. 4). (source: author himself.).

3.3.2. Differential Scanning Calorimetry (DSC). As shown in Figure 6, the energy consumption properties of NC and its precursors during pyrolysis, measured a DSC analysis between ranges of 50 to 350°C, reflect the melting point of two nanocellulose (NC) samples treated after enzymatic hydrolysis.

These showed a similar behavior, when the temperature increased above 200°C, two endothermic peaks at to 209 and 219°C were formed.

While in Figure 7, the energy consumption properties of NC and its precursors during pyrolysis, measured in analysis DSC between ranges of 50 to 350°C, are reflected. The melting point of nanocellulose obtained after acid hydrolysis showed a similar behaviour crystallizing near (207°C). The DSC study confirmed the highest crystallinity and thermal stability.

Some authors have explained that nanocellulose exhibits a three-step decomposition pattern. The first loss is ascribed to water vaporization, the second corresponding to the pyrolysis of cellulose, which involves a combination of decomposition and depolymerisation of glycosyl units, and the third stage to the degradation of carbonic residues into lower molecular weight components. Similar patterns were also reported by [23, 33] for nanocelluloses extracted from groundnut shells and rice husk, respectively.

The more intense second transition peak in the region 200–400°C occurred as a result of melting of cellulose components in the sample [24]. Theses endothermic peaks are mainly due to the formation and evaporation of levoglucosan, which is a product of cellulose depolymerisation [42]. In this respect, it has been reported that commercial cellulose contains endothermic peaks related to its crystal melting up to 330°C, and so that a decrease in the position of the peak (207–209°C) indicates an increase in the amount of amorphous cellulose [36]. Recent research has provided results that show crystallization peaks in acid hydrolysis with nanocellulose from 238°C to 273°C [25].

3.3.3. X-Ray Diffraction (XRD). Different peaks were obtained around $2\theta = 16^{\circ}$, 22° and 35°, but two main peaks at $2\theta = 16^{\circ}$ and $2\theta = 22^{\circ}$ correspond to ordered crystalline arrangements due to the formation of inter and intra molecular hydrogen bonding [4, 12]. Crystallinity is expressed as the ratio of the diffraction from a crystalline region to the total diffraction of a sample [43].

The crystallinity index was determined for various samples and the results are summarized in Table 1.

The crystallization index (CrI) was increased when acid hydrolysis was applied (28.7%) compared to untreated cellulose (15.4%) (Table 1), which is an advantage compared to enzymatic hydrolysis (20%) and untreated cellulose (10%). This result was lower than that of other researchers [44], who found a crystallization rate of up to 46% and a surface area of 5 cm 2/g with excellent thermal stability. However, [21] some have confirmed that crystallinity of the purified cellulose of rice husk and rice straw was 67% and 56%, respectively.

They assure that the removal of nanocellulosic constituents of fibers by chemical treatment causes the crystallinity to change. Treatment with alkali leads to the removal of cementing materials such as lignin, hemicelluloses, and pectin, which will result in an increase in the percentage crystallinity of the fibers [21].

The progressive increase in crystallinity was mainly due to the successive degradation and removal of lignin

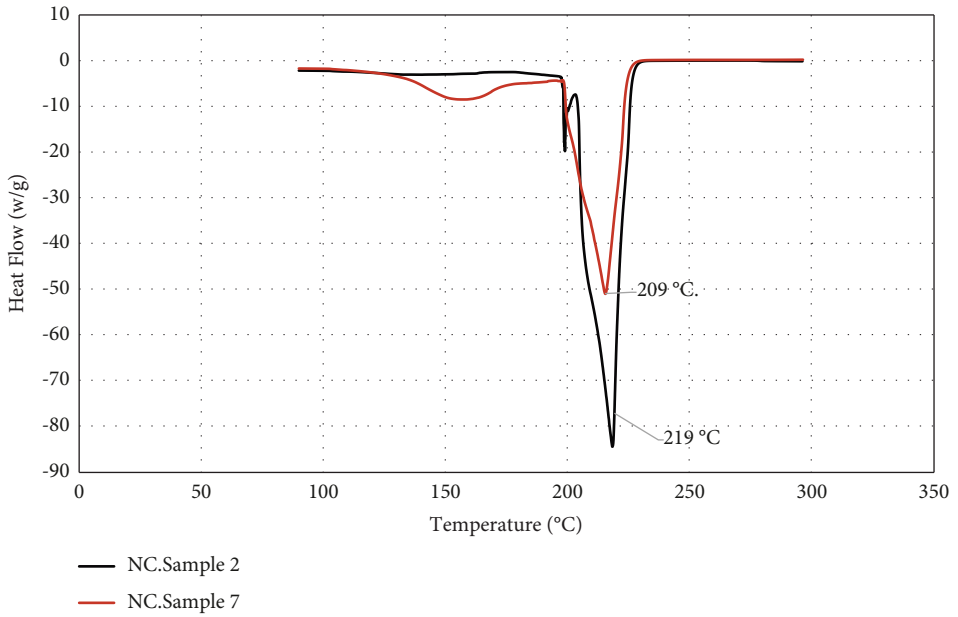

Figure 6: Differential scanning calorimetry (DSC) analysis two nanocellulose samples after enzymatic hydrolysis, that showing two peaks typical of nanocellulose. source: author himself.

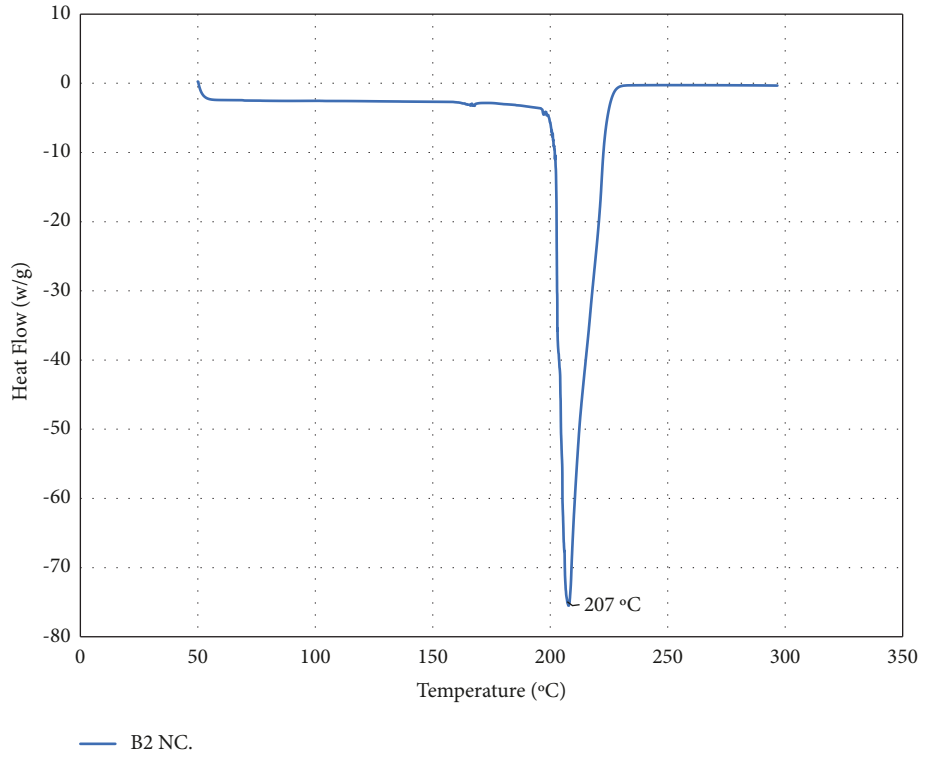

Figure 7: Differential scanning calorimetry (DSC) analysis of a sample treated (*B2*) with, showing an endothermic peak typical of nanocellulose (207°C), obtained by acid hydrolysis 64% sulfuric acid (H_2SO_4). (source: author himself).

(a cementing material) and hemicellulose from the amorphous region during acid treatment, resulting in the realignment of crystalline domains.

In the native biomass, previous analysis indicated components as follows: lignin (7.68%), hemicellulose (16.98%), silica (70.6%), and cellulose (36.8%). Therefore, we understand that according to the values of the crystallization index (CrI), from the pretreatment until later completing the hydrolysis process (acid/enzymatic), there was a loss of these molecules present in the native biomass. As shown here, the crystallinity of nanocellulose was higher (28.7–20%) than the crystallinity of unprocessed materials (15.4 –10%).

Table 1: Comparative summary of crystallinity index (CrI %) calculated, following Segal's method [4], for rice husk fibers at different stages, cellulose untreated and after used both hydrolysis.

Sample (rice husk)	CrI (%)
Untreated (A. H.)	15.4
Nanocelulosa (NC) (A.H)	28.7
Untreated (E. H)	10.0
Nanocelulosa (NC) (E.H)	20.0

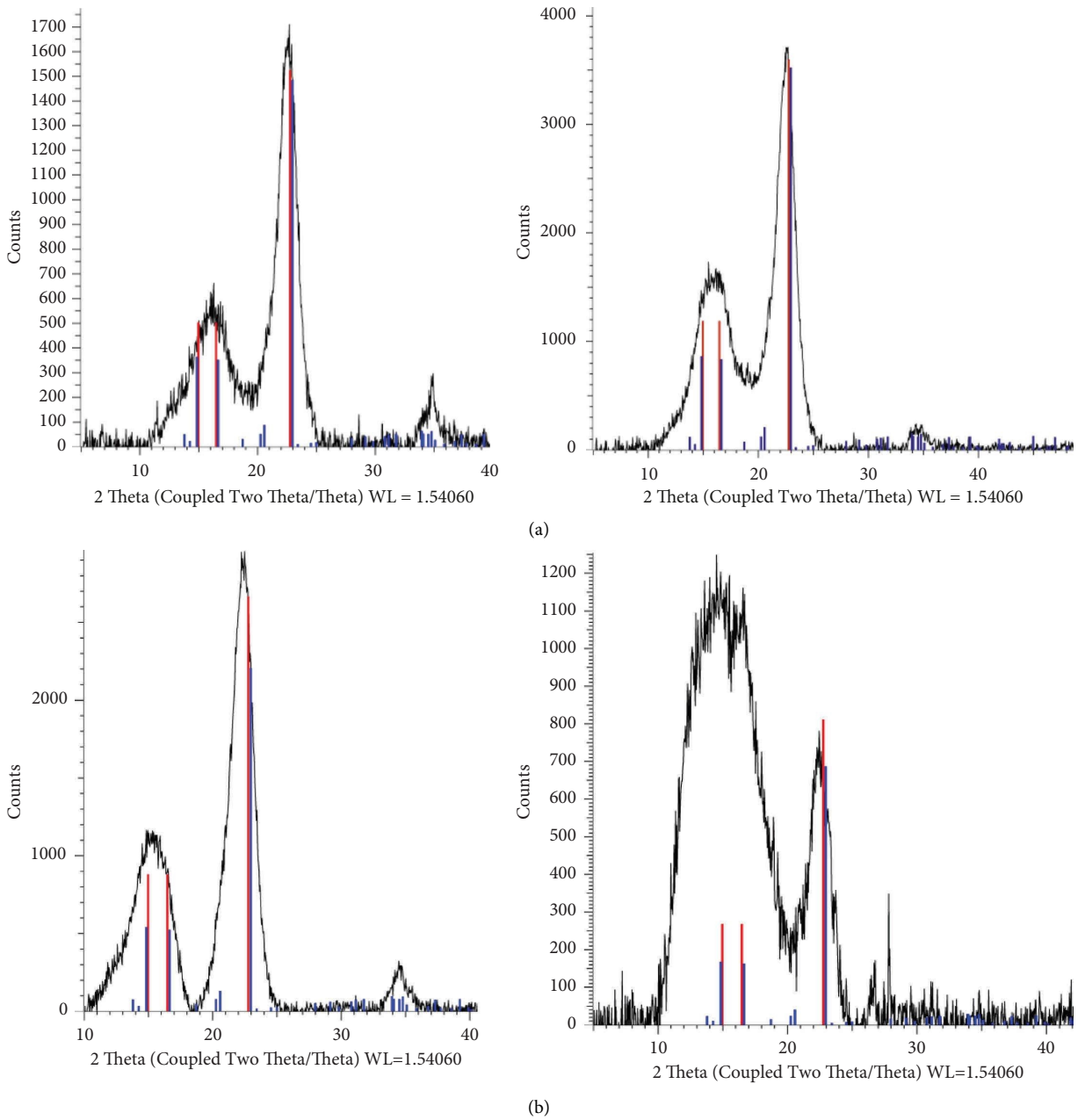

Figure 8: (a) Diffraction peaks obtained in the X-ray (XRD) analysis for three samples: original cellulose (C1), untreated, samples (C8) processed by enzymatic hydrolysis. The diffraction peaks obtained show the two highest values of crystallization formed. Author himself. (b) A sample of the diffraction peaks obtained in the X-ray diffraction (XRD) analysis for two samples: the original cellulose (B2) untreated and samples (B4) processed by acid hydrolysis. The diffraction peaks obtained show the two highest values of crystallization formed. Author himself.

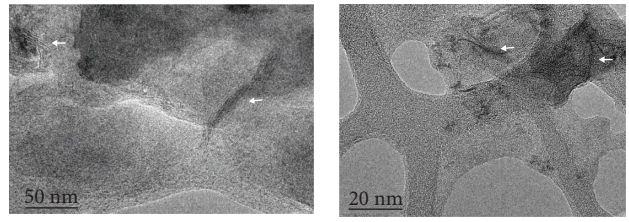

(a) (b)

Figure 9: (a) Transmission electron microscope image of NCs obtained by enzymatic hydrolysis. Nanoparticles typically have a straight rod morphology and form aggregates. Arrows point to nanocellulose groups. Line size (50 nm). Author himself. (b) Transmission electron microscope image of NCs obtained by acid hydrolysis. Nanoparticles typically have a straight rod morphology and form aggregates. Arrows point to nanocellulose groups. Line size (20 nm). Author himself.

Coinciding [45], who inferred, that higher temperatures of the thermal decomposition of the purified cellulose fibers, are related to the partial removal of hemicelluloses, lignin, and pectin from the fibers, as well as the higher crystallinity of cellulose. This is an agreement with other researchers who used rice husk [3, 10, 27].

During hydrolysis, hydronium ions penetrate into the amorphous regions of cellulose and allocate hydrolytic cleavage of glycosidic bonds, which ultimately releases individual nanocrystallites [46]. Due to an increase in the crystallinity of nanoparticles in the rice husk, stiffness, rigidity, and hence strength increase.

From the literature, it has been reported that the crystallinity of the sample increases after acid treatment [20, 47].

Diffraction patterns for (a) untreated and acid hydrolyses rice husk have been demonstrated. The X-ray studies, with crystallinity curves of pure cellulose (untreated), Nanocelulosa obtained from rice husk by acid hydrolysis and from Enzymatic hydrolysis are illustrated in Figures 8(a) and 8(b).

This confirms nanocellulose (NC) obtaining from rice husk (Figure 8(a)). Coincidentally, two important peaks (16°) and a second (22°) were obtained, which correspond to ordered crystalline arrangements due to the formation of inter and intra molecular hydrogen bonds [5, 12]. Crystallinity is expressed as the ratio of the diffraction of a crystalline region to the total diffraction of a sample [43].

In this X-ray study, it shows the crystallinity of ground rice hulls: untreated and treated by enzymatic hydrolysis (Figure 8(b)). Different peaks $2\theta = 16^\circ$, 22°, and 35° were obtained, but there were only two main peaks at $2\theta = 16^\circ$ and $2\theta = 22^\circ$ corresponding to ordered crystalline arrangements due to the formation of inter and intra molecular hydrogen bonds [5, 12]. A diffraction pattern for untreated and acid hydrolyses rice husk has been demonstrated.

3.3.4. Transmission Electron Microscopy. Figures 9(a) and 9(b) show the images as evidence formation of nanoparticles (NC) aggregates in the form of straight rods, with a length between 20–50 nm. It is confirmed that both enzymes are allowed for an easy and simple hydrolysis compared to acid hydrolysis. According to some authors [38], the formation of these aggregates is caused by the negative charges of these rods, which attract each other to form clumps.

The images shown confirm the idea that both hydrolyses produce similar sizes and shapes of nanowhiskers.

This method is an alternative to the conventional chemical pretreatments due to their low energy consumption;, it is also an ecofriendly method with negligible emission of harmful contaminants into the environment. The enzymes complex, such as cellobiose and endo-1,4-β-D-glucanase [26, 30], used in this treatment at low doses proved adequate to achieve a better nanoparticle yield. These enzymes degrade the lignin and hemicellulose regions, which further help the biodegradability of cellulose.

4. Conclusions

With a number of analytical and morphological evidence, the study supported the initial hypothesis that nanoconstructional differences exist in the husks of long grain rice variety from Morelos State and that can be used to obtained nanoparticles both methods chemical and biological.

The results obtained with pretreatment with HCl, achieved potential yields of 28 to 19% of cellulose, preferably when use waste size medium (sieved # 15 and 30), with a purity similar to the commercial standard of cellulose microcrystalline.

The bands generated in the FTIR analysis were very similar to the groups found when enzymatic hydrolysis was applied. However, some particularities regarding the nonuniformity between treatments 3 and 4 were observed when acid hydrolysis was used.

On the enzymatic pathway, there are no sharp transitions, and the peaks originating between them are very similar and soft.

Standing out were the peaks formed at 2920 cm^{-1} and 1650 cm^{-1} with greater bound water with sieves # 30 and 50 in the production of cellulose.

Although the use of enzymatic hydrolysis to obtain nanocellulose from rice husk biomass has been little discussed, it was found that cellobiose and endo-1,4-β-D-glucanase can be used in a more beneficial, simple, and reliable process that is also less expensive than acid hydrolysis, without excessive energy expenditure, and only two enzymes are taken into account.

The X-ray studies show two important peaks, the first (16°) and a second (22°), which corresponds to ordered crystalline arrangements in the formation of nanocellulose

by both hydrolysis ways. Time longer process, but with less environmental aggression were appreciated than acid hydrolysis. Although the crystallization index (CrI) was increased, acid hydrolysis was applied, compared to untreated cellulose, which is an advantage compared to enzymatic hydrolysis.

The peaks obtained between 207, 208, and 209°C by action of both hydrolysis permit explain, more accurate to describe the increase in amorphous cellulose formed.

The formation and size of the nanoparticles, by both hydrolysis procedures, give rise to typical straight elongated rods, with a size between 20–50 nm, which form aggregates, given their electrical charges.

Data Availability

All data have been included in the manuscript.

Conflicts of Interest

The authors declare that they have no conflicts of interest.

Acknowledgments

To General Direction of TecNM/ITZacatepec, for support the execution of the project. Also, the authors thank Dr. Efraín Rubio-Rosas from University Center for Linkage and Technology Transfer, Meritorious Autonomous, Puebla University, Puebla, Mexico.

References

[1] P. Manzanares, "The role of biorefinering research in the development of a modern bioeconomy," *Acta Innovations*, vol. 37, pp. 47–56, 2020.

[2] Y. T. Xiao, W. L. Chin, and S. B. Abd Hamid, "Facile preparation of highly crystalline nanocellulose by using ionic liquid," *Advanced Materials Research*, vol. 1087, pp. 106–110, 2015.

[3] J. Vargas, P. Alvarado, J. Vega-Baudrit, and M. Porras, "Caracterización de subproducto cascarillas de arroz en búsqueda de posibles aplicaciones como materia prima en procesos," *Rev. Científica. Univ. Costa Rica*, vol. 23, no. 1, pp. 86–101, 2013.

[4] J. Lgjma Segal, A. Martin, and C. Conrad, J. Creely, "An empirical method for estimating the degree of crystallinity of native cellulose using the X-ray diffractometer," *Textile Research Journal*, vol. 29, no. 10, pp. 786–794, 1959.

[5] J. C. Cs, N. George, and S. K. Narayanankutty, "Isolation and characterization of cellulose nanofibrils from arecanut husk fibre," *Carbohydrate Polymers*, vol. 142, pp. 158–166, 2016.

[6] S. Kumagai and J. Sasaki, "Carbon/silica composite fabricated from rice husk by means of binderless hot-pressing," *Bioresource Technology*, vol. 100, no. 13, pp. 3308–3315, 2009.

[7] A. Frenot, M. W. Henriksson, and P. Walkenström, "Electrospinning of cellulose-based nanofibers," *Journal of Applied Polymer Science*, vol. 103, no. 3, pp. 1473–1482, 2007.

[8] A. Maleki, H. Movahed, and P. Ravaghi, "Magnetic cellulose/Ag as a novel eco-friendly nanobiocomposite to catalyze synthesis of chromene-linked nicotinonitriles," *Carbohydrate Polymers*, vol. 156, pp. 259–267, 2017.

[9] Y. Zhou, C. Fuentes-Hernández, T. M. Khan et al., "Recyclable organic solar cells on cellulose nanocrystal substrates," *Scientific Reports*, vol. 3, no. 1, p. 1536, 2013.

[10] N. Johar, I. Ahmad, and A. Dufresne, "Extraction, preparation and characterization of cellulose fibres and nanocrystals from rice husk," *Industrial Crops and Products*, vol. 37, no. 1, pp. 93–99, 2012.

[11] K. G. Satyanarayana, G. G. C. Arizaga, and F. Wypych, "Biodegradable composites based on lignocellulosic fibers—an overview," *Progress in Polymer Science*, vol. 34, no. 9, pp. 982–1021, 2009.

[12] W. P. Flauzino Neto, H. A. Silvério, N. O. Dantas, and D. Pasquini, "Extraction and characterization of cellulose nanocrystals from agro-industrial residue – soy hulls," *Industrial Crops and Products*, vol. 42, pp. 480–488, 2013.

[13] A. Champión-Coria, A. A. Castillo, O. S. Martínez, J. C. T. Picazo, A. V. González, and P. J. H. Franco, "Acabado superficial en fibras de carbón mediante análisis de Hurst," *Rev. Iberoam. Polym*, vol. 13, pp. 151–157, 2012.

[14] L. Jiang, E. Morelius, J. Zhang, M. Wolcott, and J. Holbery, "J, study of the poly (3-hydroxybutyrate-co-3-hy- droxyvalerate)/cellulose nanowhisker composites prepared by solution casting and melt processing," *Journal of Composite Materials*, vol. 42, pp. 2629–2645, 2008.

[15] B. E. Urena, "Cellulose nanocrystals properties and applications in renewable nanocomposites," *All Dissertations*, vol. 704, pp. 1–169, 2011.

[16] S. Maiti, J. Jayaramudu, K. Das et al., "Preparation and characterization of nano-cellulose with new shape from different precursor," *Carbohydrate Polymers*, vol. 98, no. 1, pp. 562–567, 2013.

[17] E. Guilbert-García, R. Salgado-Delgado, N. A. Rangel-Vázquez, E. García-Hernández, E. Rubio-Rosas, and R. Salgado-Rodríguez, "Modification of rice husk to improve the interface in isotactic polypropylene composites," *Latin American Applied Research*, vol. 42, pp. 83–87, 2012.

[18] N. Hayashi, T. Kondo, and M. Ishihara, "Enzymatically produced nano-ordered short elements containing cellulose Iβ crystalline domains," *Carbohydrate Polymers*, vol. 61, no. 2, pp. 191–197, 2005.

[19] S. Iwamoto, W. Kai, T. Isogai, T. Saito, A. Isogai, and T. Iwata, "Comparison study of TEMPO-analogous compounds on oxidation efficiency of wood cellulose for preparation of cellulose nanofibrils," *Polymer Degradation and Stability*, vol. 95, no. 8, pp. 1394–1398, 2010.

[20] L. G. Tang, D. N. S. Hon, S. H. Pan, Y. Q. Zhu, Z. Wang, and Z. Z. Wang, "Evaluation of microcrystalline cellulose. I. Changes in ultrastructural characteristics during preliminary acid hydrolysis," *Journal of Applied Polymer Science*, vol. 59, no. 3, pp. 483–488, 1996.

[21] S. Rezanezhad, N. Nazanezhad, and G. Asadpur, "Solation of nanocellulose from rice waste via ultrasonication," *Lignocellulose*, vol. 2, pp. 282–291, 2013.

[22] M. I. Hossain, H. Zaman, and T. Rahman, "Derivation of nanocellulose from native rice husk," *Chemical Engineering Research Bulletin*, vol. 20, no. 1, pp. 19–22, 2018.

[23] M. Kaur, S. Kumari, and P. Sharma, "Chemically modified nanocellulose from rice husk: synthesis and characterisation," *Advances in Research*, vol. 13, no. 3, pp. 1–11, 2018.

[24] S. M. L. Rosa, N. Rehman, M. I. G. de Miranda, S. M. Nachtigall, and C. I. D. Bica, "Chlorine-free extraction of cellulose from rice husk and whisker isolation," *Carbohydrate Polymers*, vol. 87, no. 2, pp. 1131–1138, 2012.

[25] R. Hernández Pérez, A. Olarte Paredes, R. Salgado Delgado, and A. M. Salgado Delgado, "Rice husk Var. 'Morelos A-2010' as an eco-friendly alternative for the waste management converting them cellulose and nanocellulose," *International Journal of Environmental Analytical Chemistry*, vol. 101, pp. 1–16, 2021.

[26] R. P. Hernández, A. C. Álvarez, A. P. Olarte, and A. M. D. Salgado, "Manejo de la cascarilla de arroz como residuo postcosecha y su conversión en nanocelulosa," *Mundo Nano*, vol. 16, p. 30, 2023.

[27] L. V. Peñaranda Gonzalez, S. P. Montenegro Gómez, P. A. Giraldo Abad, and A. P. Giraldo, "Aprovechamiento de residuos agroindustriales en Colombia," *Rev. Investig. Agrar. Ambient*, vol. 8, no. 2, pp. 141–150, 2017.

[28] S. Gowthaman, K. Nakashima, and S. Kawasaki, "A state-of-the-art review on soil reinforcement Technology using natural plant fiber materials: past findings, present trends and future directions," *Materials*, vol. 11, no. 4, p. 553, 2018.

[29] B. L. Peng, N. Dhar, H. L. Liu, and K. C. Tam, "Chemistry and applications of nanocrystalline cellulose and its derivatives: a nanotechnology perspective," *Canadian Journal of Chemical Engineering*, vol. 89, no. 5, pp. 1191–1206, 2011.

[30] C. Zinge and B. Kandasubramanian, "Nanocellulose based biodegradable polymers," *European Polymer Journal*, vol. 133, p. 109758, Article ID 109758, 2020.

[31] Y. Zhao, Z. Qiu, W. Yang, R. K. Yuen, and R. K. Y. Li, "Effect of multi-walled carbon nanotubes on the crystallization and hydrolytic degradation of biodegradable poly(l-lactide)," *Composites Science and Technology*, vol. 69, no. 5, pp. 627–632, 2009.

[32] S. Rashid and H. Dutta, "Characterization of nanocellulose extracted from short, medium and long grain rice husks," *Industrial Crops and Products*, vol. 154, Article ID 112627, 2020.

[33] D. A. Onoja, I. Ahemen, and T. F. Iorfa, "Synthesis and characterization of cellulose based nanofibers from rice husk," *IOSR Journal of Applied Physics*, vol. 11, pp. 80–87, 2019.

[34] V. Nang An, H. T. Chi Nhan, T. D. Tap, T. T. T. Van, P. Van Viet, and L. Van Hieu, "Extraction of high crystalline nanocellulose from biorenewable sources of Vietnamese agricultural wastes," *Journal of Polymers and the Environment*, vol. 28, no. 5, pp. 1465–1474, 2020.

[35] J. P. d. Oliveira, G. P. Bruni, K. O. Lima et al., "Cellulose fibers extracted from rice and oat husks and their application in hydrogel," *Food Chemistry*, vol. 221, pp. 153–160, 2017.

[36] J. I. Morán, V. A. Alvarez, V. P. Cyras, and A. Vázquez, "Extraction of cellulose and preparation of nanocellulose from sisal fibers," *Cellulose*, vol. 15, no. 1, pp. 149–159, 2008.

[37] A. L. M. P. Leite, C. D. Zanon, and F. C. Menegalli, "Isolation and characterization of cellulose nanofibers from cassava root bagasse and peelings," *Carbohydrate Polymers*, vol. 157, pp. 962–970, 2017.

[38] Q. Liu, Y. Lu, M. Aguedo et al., "Isolation of high-purity cellulose nanofibers from wheat straw through the combined environmentally friendly methods of steam explosion, microwave-assisted hydrolysis, and microfluidization," *ACS Sustainable Chemistry & Engineering*, vol. 5, no. 7, pp. 6183–6191, 2017.

[39] S. L. M. El Halal, R. Colussi, V. G. Deon et al., "Films based on oxidized starch and cellulose from barley," *Carbohydrate Polymers*, vol. 133, pp. 644–653, 2015.

[40] R. Salgado-Delgado, S. R. Vázquez, A. Alvarez-Castillo, A. Licea-Claverie, and V. M. Casiaño, "Chemical modification of rice husk surface through alkaline treatments," *Materials Technology*, vol. 20, no. 1, pp. 26–29, 2005.

[41] A. Mandal and D. Chakrabarty, "Isolation of nanocellulose from waste sugarcane bagasse (SCB) and its characterization," *Carbohydrate Polymers*, vol. 86, no. 3, pp. 1291–1299, 2011.

[42] S. Soares, G. Camino, and S. Levchik, "Comparative study of the thermal decomposition of pure cellulose and pulp paper," *Polymer Degradation and Stability*, vol. 49, no. 2, pp. 275–283, 1995.

[43] A. Alemdar and M. Sain, "Isolation and characterization of nanofibers from agricultural residues – wheat straw and soy hulls," *Bioresource Technology*, vol. 99, no. 6, pp. 1664–1671, 2008.

[44] S. F. Adil, S. V. Bhat, K. M. Batoo et al., "A. Isolation and characterization of nanocrystalline cellulose from flaxseed Hull: a future onco-drug delivery agent," *Journal of Saudi Chemical Society*, vol. 24, pp. 374–379, 2020.

[45] K. Abe, S. Iwamoto, and H. S. Yano, "Obtaining cellulose nanofibers with a uniform width of 15 nm from wood," *Biomacromolecules*, vol. 8, no. 10, pp. 3276–3278, 2007.

[46] M. M. de Souza Lima, R. Borsali, and R. Borsali, "Rodlike cellulose microcrystals: structure, properties, and applications," *Macromolecular Rapid Communications*, vol. 25, no. 7, pp. 771–787, 2004.

[47] M. A. S. Azizi Samir, F. Alloin, and A. Dufresne, "Review of recent research into cellulosic whiskers, their properties and their application in nanocomposite field," *Biomacromolecules*, vol. 6, no. 2, pp. 612–626, 2005.